

Acid- and Base-Stable Porous Organic Cages: Shape Persistence and pH Stability via Post-synthetic “Tying” of a Flexible Amine Cage

Ming Liu, Marc A. Little, Kim E. Jelfs,[‡] James T. A. Jones,[§] Marc Schmidtman, Samantha Y. Chong, Tom Hasell, and Andrew I. Cooper*

Department of Chemistry and Centre for Materials Discovery, University of Liverpool, Liverpool L69 7ZD, U.K.

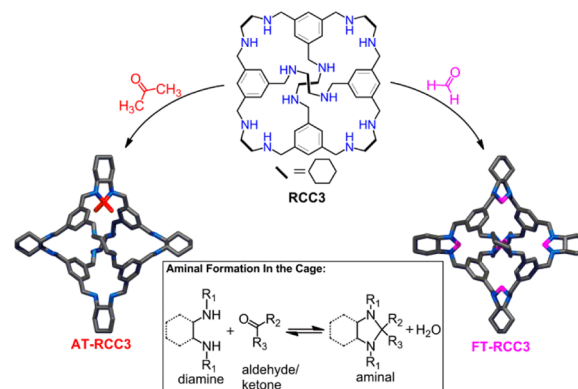
S Supporting Information

ABSTRACT: Imine cage molecules can be reduced to amines to improve their chemical stability, but this introduces molecular flexibility. Hence, amine cages tend not to exhibit permanent solid-state porosity. We report a synthetic strategy to achieve shape persistence in amine cages by tying the cage vertices with carbonyls such as formaldehyde. Shape persistence is predicted by conformer stability calculations, providing a design basis for the strategy. The tied cages show enhanced porosity and unprecedented chemical stability toward acidic and basic conditions (pH 1.7–12.3), where many other porous crystalline solids would fail.

Schiff-base chemistry is one of the most versatile methods for the construction of organic macrocycles and cages.¹ The reversibility of the imine bond-forming reaction gives a route to thermodynamically equilibrated products. This has been used to produce crystalline porous organic solids, such as covalent organic frameworks (COFs)² and porous molecular organic cages.³ In particular, a series of porous, shape-persistent imine cages has been reported,⁴ and surface areas as high as 3758 m²/g have been attained,⁵ thus rivaling extended frameworks such as metal–organic frameworks (MOFs).⁶ Porous molecular organic solids show promise as adsorbents for radioisotope pollutants,⁷ as molecular additives in organic–organic mixed-matrix membranes,⁸ as shape-selective chromatography phases,⁹ and as materials for molecular sensing.¹⁰

However, the reversibility of imine chemistry, which permits equilibrium products to form, can also cause problems of chemical instability, thus limiting its wider application. Imines are prone to hydrolysis and can decompose upon exposure to atmospheric moisture, although there are some exceptions to this.^{2,11} Imines are even more prone to hydrolysis in acidic or basic environments. A straightforward way to make an imine more chemically stable is to reduce it to the corresponding amine. In addition to enhancing chemical stability, amine cages are also readily functionalized¹² and can provide binding sites for guests such as CO₂.¹³ However, while many amine cages and macrocycles have been reported via imine reduction, no truly shape-persistent porous amine cages have been discovered. This is because reduction to the amine introduces additional flexibility in the cage molecule, and this leads to loss of the internal cavity, or pore. We previously reported a [4+6] amine cage formed by reduction of the equivalent imine cage, CC1, but crystallization attempts yielded only amorphous, nonporous solids for the

Scheme 1. Synthesis of “Tied” Porous Cages



amine derivative.¹⁴ Zhang et al. reported a series of [2+3] amine cages, but these, too, collapsed in the absence of solvent, and a very low level of porosity (but a high CO₂/N₂ selectivity) was observed.¹⁵ Mastalerz et al. reduced their [4+6] salicylbisimine cages to the corresponding amines, but this also resulted in a collapse of the cage, loss of the intrinsic cage cavity, and a dramatic decrease in porosity.^{10,16} These examples all demonstrate that the increased flexibility of saturated amine bonds with respect to unsaturated imine bonds causes loss of shape persistence in the molecule, even when the parent imine cage is shape-persistent and porous.

Here we report a protocol to stabilize flexible amine cages and to produce shape-persistent, chemically stable amines that are porous in the solid state. The shape persistence of the parent imine cage is regained by reaction with a suitable “tie” molecule on the cage vertices. Remarkably, the tied porous crystal is highly stable, even to prolonged treatment in acid or base.

The amine cage that we investigated was RCC3 (Scheme 1), a reduced derivative of the parent, chiral imine cage, CC3, which has tetrahedral symmetry (point group *T*) and is formed by cycloimination of 1,3,5-triformylbenzene and (1*R*,2*R*)-1,2-diaminocyclohexane.^{3a} CC3 is readily prepared on a large scale (>100 g) in a one-pot condensation reaction, and it has an apparent Brunauer–Emmett–Teller (BET) surface area of ~400 m²/g in highly crystalline form.¹⁷ CC3 was reduced to the corresponding dodecaamine cage, RCC3, by treatment with NaBH₄ in close to 100% yield. Single-crystal X-ray diffraction (SC-XRD) for a solvated crystal of RCC3 revealed that the

Received: April 4, 2014

Published: May 2, 2014

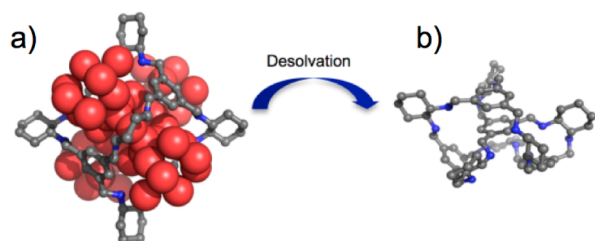


Figure 1. (a) Single-crystal structure of **RCC3** solvate, with H_2O /methanol guests shown in red. (b) Representative energy-minimized model of a collapsed, desolvated **RCC3** amine cage.

molecule retains the tetrahedral shape of the parent imine cage, **CC3**, providing that methanol and H_2O guests fill the pores in the structure (Figure 1a). The more flexible amine bonds in **RCC3** are no longer planar with the adjacent benzene ring, as for **CC3**, but point away from the cage cavity at an angle of 10° from the benzene plane. **RCC3** packs in a window-to-window fashion, like the imine cage **CC3**. This could, in theory, produce an isostructural interconnected diamondoid pore network, with the cage molecules acting as tetrahedral nodes. However, multiple attempts to desolvate **RCC3** by slow drying, solvent exchange, or supercritical fluid drying all resulted in amorphous solids (Supporting Information (SI), Figure S1). Unlike **CC3**, desolvated **RCC3** did not exhibit any porosity to either N_2 or H_2 at 77 K, or to CO_2 at 298 K. By contrast, **CC3** is also porous in the amorphous state—more porous, in fact, than in its crystalline form.¹⁷ We thus ascribe the loss of porosity in **RCC3** to collapse of its flexible cage cavity upon desolvation, rather than to it being amorphous.

We previously used computational conformer searching to predict the size and conformation of molecular imine cages.¹⁸ Here, we use this approach to investigate the shape persistence of various amine cages. For **RCC3**, conformer searches confirmed the collapse of the molecular structure, with multiple possible collapsed conformations within a few kJ/mol of each other, all lying significantly lower (>100 kJ/mol) in energy than the open void conformation that is stabilized by solvent in the **RCC3** solvate (Figure 1a). A representative example of a collapsed **RCC3** conformation is shown in Figure 1b, where the flexibility of the amine cage allows one arene face to “fold” into the cage cavity, and thus to occupy the original void space.

RCC3 is readily soluble in acetone. Surprisingly, we observed the spontaneous formation of prism-shaped single crystals from acetone solutions of **RCC3** after ~ 30 min. All characterization data suggested that just one of the six diamine vertices on each **RCC3** cage had reacted with acetone to afford a new molecule, **AT-RCC3** (where AT = “acetone tied”), by forming a 5-member imidazolidine (aminal) ring (Scheme 1). The geometry of the chiral (1*R*,2*R*)-1,2-diaminocyclohexanediamine in **RCC3** promotes formation of a 5-member imidazolidine ring. This is consistent with previous reports of aminal formation from secondary diamines and carbonyls.¹⁹ **AT-RCC3** crystallizes in the chiral cubic space group $F4_132$, like **CC3**,^{3a} with comparable cell parameters. SC-XRD reveals that **AT-RCC3** has tetrahedral symmetry and that the single imidazolidine ring is disordered over the six diamine vertices. To confirm that no further diamine vertices could be functionalized, this “reactive recrystallization” was repeated at higher temperature (50°C) using a cosolvent ($\text{CHCl}_3/\text{acetone}$, 1:1 v/v) for 24 h; again, reaction occurred at just one diamine vertex. We believe that the first acetone “tie” prevents a second acetone molecule from reacting in the cage,

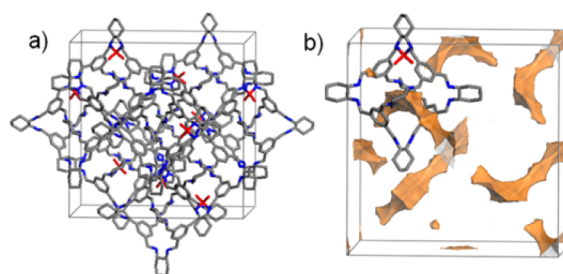


Figure 2. (a) Crystal packing for shape-persistent **AT-RCC3**. Ties are shown in red, C in gray, N in blue, and H omitted. The ties were positionally disordered (randomized) in this structural model. (b) Solvent-accessible surface for **AT-RCC3** generated using a probe radius of 1.82 \AA for N_2 using Zeo++.²⁰ A single **AT-RCC3** molecule is shown. The formally disconnected voids are shown in orange. The acetone tie blocks its two neighboring windows for the N_2 probe in each cage.

probably by steric inhibition of intermediates (SI, Scheme S1). The solubility of **AT-RCC3** in acetone was also significantly decreased compared with that of **RCC3**, and **AT-RCC3** precipitated from solution upon formation. This drives the reversible aminal formation reaction by removing the aminal product from equilibrium, explaining the almost 100% conversion of **RCC3** to **AT-RCC3**. As a side benefit, this reversible acetone/**RCC3** reaction constitutes a simple and effective method to purify **RCC3** by forming the aminal, filtering, redissolving, and reversing the aminal reaction to regenerate the amine cage, **RCC3** (SI sections 1.8 and 1.9, Figure S5).

AT-RCC3 forms reversibly in solution (SI section 1.8), providing an effective method for purifying **RCC3**, as described in the ESI (1.9). However, the crystalline solvate of **AT-RCC3** is stable in the solid state up to around 300°C and also to immersion in water for 48 h.

Like **CC3**, desolvated **AT-RCC3** packs in a window-to-window fashion (Figure 2a). Gas adsorption analysis for desolvated **AT-RCC3** (Figure 3a) showed that the material adsorbs a very modest amount of N_2 (1.11 mmol/g) and H_2 (1.29 mmol/g) at 77 K and 1 bar. The apparent BET surface area was just $67 \text{ m}^2/\text{g}$, as calculated from the N_2 isotherm. This surface area and gas uptake are substantially lower than for isostructural **CC3**.^{3a} However, close to ambient temperature, a CO_2 uptake of 1.77 mmol/g was observed for **AT-RCC3**—that is, 8 times higher than for **RCC3** (Figure 3b). The ideal gas selectivity for CO_2/N_2 was calculated as 57 at 298 K and 1 bar. This is close to the CO_2/N_2 selectivity of the [2+3] imine cages reported by Zhang et al.,¹⁵ but with a much higher absolute CO_2 uptake (1.77 mmol/g for **AT-RCC3** vs $0.1\text{--}0.25 \text{ mmol/g}$ for the Zhang cages). The lack of N_2 and H_2 adsorption at low temperature in **AT-RCC3** is explained by its crystal structure. The solvent-accessible surface with a N_2 probe radius of 1.82 \AA ²¹ shows formally disconnected voids (Figure 2b). This is because the dimethyl groups block two of the four windows on each **AT-RCC3** cage. The interconnectivity of the pore structure for N_2 thus depends upon the spatial arrangement of these dimethyl-blocked windows with respect to one another.

This disconnects the pore volume (Figure 2b), particularly at low temperatures where molecular motion and dynamic cooperative diffusion are less prevalent. At higher temperatures, it is possible that thermal motion allows gases to negotiate these blocked pathways. The five remaining unreacted diamine groups per cage molecule may promote CO_2 adsorption;^{13,22} this could account, in part, for the high CO_2/N_2 selectivity in **AT-RCC3**.

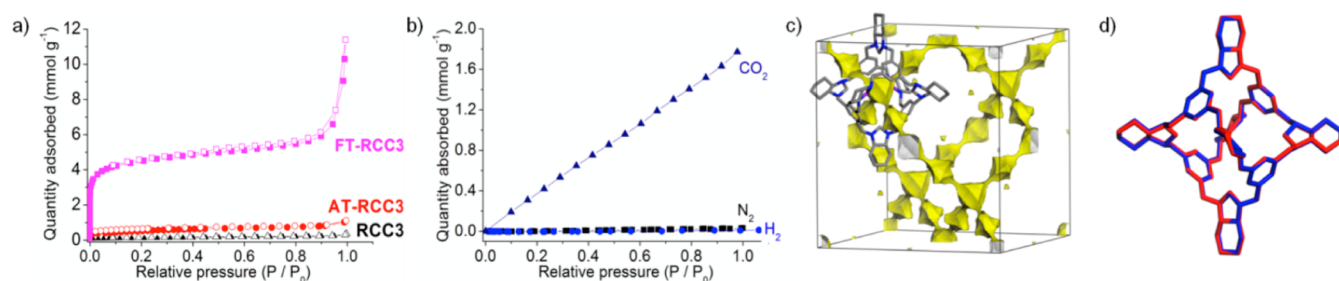


Figure 3. (a) N_2 adsorption/desorption isotherms at 77 K showing a substantial increase in porosity for FT-RCC3 vs AT-RCC3 and RCC3. Solid symbols, adsorption; open symbols, desorption. (b) CO_2 (navy triangles), N_2 (black squares), and H_2 (blue circles) adsorption isotherms for AT-RCC3 at 298 K. (c) Solvent-accessible surface for FT-RCC3 using a probe radius of 1.42 Å for H_2 , showing an interconnected 3D diamondoid pore network. (d) Overlay of the calculated lowest energy structure (red) and SC-XRD structure for a solvate of FT-RCC3 (blue; solvent molecules omitted for clarity, see SI, section 1.19).

Reaction with a single acetone rigidifies the amine cage relative to RCC3, but AT-RCC3 is still too flexible to retain permanent porosity over a time scale of days. As shown in Figure S6, a slight loss in crystalline order was observed after desolvation, and a further loss of crystallinity was apparent after gas sorption analysis. In addition, after exposing AT-RCC3 to CO_2 (5 bar), we found evidence for a second single-crystal phase, not evident in the as-synthesized material. This phase comprised a collapsed conformation of AT-RCC3 where the imidazolidine ring preferentially collapses into the cage cavity (SI, section 1.12, Figure S7). Improved shape persistence might be expected if we tied all six diamine vertices, rather than just one, but this rules out bulky tie molecules because they cannot react at all six diamine sites due to space constraints and bulky ties will occupy too much of the void space, and hence eliminate porosity.

The obvious candidate “tie” was formaldehyde because it is the smallest carbonyl molecule and it is highly reactive. A white precipitate formed immediately when RCC3 and paraformaldehyde were mixed together at 70 °C in methanol. FT-RCC3 (where FT = formaldehyde tied) was recovered in 70% yield after washing with methanol and drying. NMR spectroscopy of the product suggested that all six diamine groups in RCC3 had reacted with formaldehyde, as also proven by SC-XRD (Figure 3c,d).

FT-RCC3 retains the tetrahedral symmetry of the imine, CC3, and crystallizes in $F4_132$ with similar cell parameters (Table 1).

Table 1. Unit Cell Parameters for Cages ($T = 100$ K)

	CC3	RCC3	AT-RCC3	FT-RCC3
a (Å)	25.016(2)	25.71(1)	25.469(1)	25.316(2)
V (Å ³)	15090(12)	16999(13)	16520(2)	16225(2)

The FT-RCC3 material can be fully desolvated under dynamic vacuum for 12 h at 80 °C. Unlike AT-RCC3, there was no indication of any loss of crystallinity for FT-RCC3 after either desolvation or after gas adsorption, a promising indicator of increased shape persistence (Figures S10 and S11). The porous nature of FT-RCC3 was next probed by N_2 , H_2 , and CO_2 adsorption. Nitrogen adsorption measurements at 77 K showed a Type I isotherm (Figure 3a), with a total gas uptake of 11.2 mmol/g at 1.0 bar and an apparent BET surface area of 377 m²/g. This is only slightly lower than the 409 m²/g measured for the parent imine cage, CC3.¹⁷ However, both materials have precisely the same “molar” BET surface area of 457 m²/mmol when their molecular weights are considered. FT-RCC3 adsorbs 4.3 mmol/g of H_2 at 77 K and 1.0 bar, and 1.42 mmol/g of CO_2 at

298 K and 1 bar. As can be seen from the calculated solvent-accessible surface (Figure 3c), the pores in FT-RCC3 are interconnected for a 1.42 Å H_2 probe. This interconnectivity persists for a smaller 1.55 Å probe (equivalent to a N_2 molecule oriented end-on) but becomes formally disconnected for a N_2 van der Waals radius probe of 1.82 Å. We assume that breathing motions of the molecule allow for diffusion of N_2 through the pore structure, as observed for CC3.²³

A conformational search for FT-RCC3 found that the lowest energy conformer was the observed shape-persistent structure, comprising a permanent void (Figure 2d). A partially folded conformation (Figure S12) was also found to lie 22 kJ/mol higher in energy, as calculated with the OPLS-AA force field.²⁴ DFT calculations (see SI for full details) confirmed that the open structure was indeed the lowest energy molecular structure, with an energy gap of 14 kJ/mol. An overlay of the calculated molecular structure with the experimental structure (Figure 3d) shows excellent agreement, with RMSD = 0.079 Å (excluding H's).

Most imine-based molecules are unstable in acidic or basic environments, or even in the presence of neutral water. The crystalline parent imine cage, CC3, is surprisingly robust to neutral water,¹¹ but it decomposes rapidly when immersed in mildly acidic solutions.

FT-RCC3 showed excellent stability toward water and also to both acids and bases. There was no loss of crystallinity, nor any chemical decomposition, when solid FT-RCC3 was soaked in either acidic (pH 1.7; Figure 4a) or basic (pH 12.3; Figure S13) solutions for 12 days. Likewise, these acid/base treatments did not affect the porosity in the material, as shown by the N_2 isotherms after treatment (Figure 4b). This stability also translates to FT-RCC3 in solution. For example, we found that FT-RCC3 can bind benzoic acid in $CHCl_3$ solution with an association constant of $9.1 \times 10^3 M^{-1}$. No sign of decomposition in the tied cage was observed after 10 days in this acidic solution (SI section 1.17, Figures S14–S17). Such host–guest binding in acidic media would be impossible for the imine cage, CC3. The inner cavity of FT-RCC3 becomes more hydrophobic compared with RCC3 after decoration with six methylene groups, but FT-RCC3 can still bind or adsorb polar guests such as water or benzoic acid. We thus ascribe the enhanced stability of FT-RCC3 to its more robust chemical bonding, rather than to simple exclusion of the acid or base species from the molecular pores.

In summary, we demonstrate a new protocol for stabilizing flexible amine cages. By tying the cage vertices with small carbonyl molecules, the shape persistence of the cage can be greatly improved. We illustrate this here using reactions between

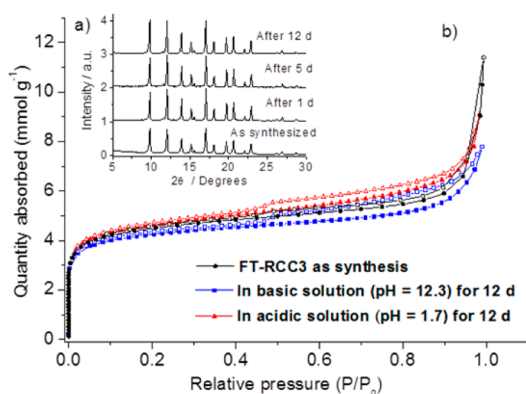


Figure 4. (a) PXRD patterns for FT-RCC3 after immersion in 0.02 M HCl (pH 1.7) for 12 days. (b) N_2 isotherms at 77 K as synthesized (black circles), and after treatment with basic (blue squares) or with acidic solution for 12 days (red triangles). Solid symbols show adsorption and open symbols desorption.

diamines and ketones or aldehydes, and the reaction is potentially transferable to other cages prepared from vicinal diamine building blocks.⁷ By choosing suitable ties, molecular collapse can be prevented, and permanent solid-state porosity can be retained. When formaldehyde is used as the tie, the resulting molecule has far better physicochemical stability than the parent imine cage. This strategy could have important practical applications. Some amorphous porous materials, such as activated carbon and porous organic polymers,²⁵ are stable to both acids and bases. By contrast, crystalline porous solids are rarely stable over such a broad pH range: most zeolites, MOFs, and COFs are attacked by either acids or bases, or both. As such, FT-RCC3 exhibits a level of chemical and crystal stability that is so far unmatched by other crystalline molecular “organic zeolites”.

■ ASSOCIATED CONTENT

📄 Supporting Information

Full synthetic and experimental details, gas adsorption data, and computational details. This material is available free of charge via the Internet at <http://pubs.acs.org>.

■ AUTHOR INFORMATION

✉ Corresponding Author

aicooper@liv.ac.uk

📍 Present Addresses

[‡]Department of Chemistry, Imperial College London

[§]Defense Science and Technology Laboratory, Salisbury, UK

📝 Notes

The authors declare no competing financial interest.

■ ACKNOWLEDGMENTS

We thank the Engineering and Research Council (EPSRC) for financial support under grant EP/H000925/1. A.I.C. is a Royal Society Wolfson Research Merit Award holder, and K.E.J. holds a Royal Society University Research Fellowship. We thank Rob Clowes for assistance with adsorption measurements. The authors thank Diamond Light Source for access to beamline I19 (MT8728) that contributed to the results presented here.

■ REFERENCES

(1) Belowich, M. E.; Stoddart, J. F. *Chem. Soc. Rev.* **2012**, *41*, 2003.

(2) Uribe-Romo, F. J.; Hunt, J. R.; Furukawa, H.; Klöck, C.; O’Keeffe, M.; Yaghi, O. M. *J. Am. Chem. Soc.* **2009**, *131*, 4570.

(3) (a) Tozawa, T.; Jones, J. T.; Swamy, S. I.; Jiang, S.; Adams, D. J.; Shakespeare, S.; Clowes, R.; Bradshaw, D.; Hasell, T.; Chong, S. Y.; Tang, C.; Thompson, S.; Parker, J.; Trewin, A.; Bacsá, J.; Slawin, A. M.; Steiner, A.; Cooper, A. I. *Nat. Mater.* **2009**, *8*, 973. (b) Mastalerz, M. *Angew. Chem., Int. Ed.* **2010**, *49*, 5042. (c) Jin, Y.; Zhu, Y.; Zhang, W. *CrystEngComm* **2013**, *15*, 1484.

(4) Jones, J. T.; Hasell, T.; Wu, X.; Bacsá, J.; Jelfs, K. E.; Schmidtman, M.; Chong, S. Y.; Adams, D. J.; Trewin, A.; Schiffman, F.; Cora, F.; Slater, B.; Steiner, A.; Day, G. M.; Cooper, A. I. *Nature* **2011**, *474*, 367. (b) Mastalerz, M. *Chem. Eur. J.* **2012**, *18*, 10082. (c) Mastalerz, M.; Schneider, M. W.; Oppel, I. M.; Presly, O. *Angew. Chem., Int. Ed.* **2010**, *50*, 1046.

(5) Zhang, G.; Presly, O.; White, F.; Oppel, I. M.; Mastalerz, M. *Angew. Chem., Int. Ed.* **2014**, *53*, 1516.

(6) Farha, O. K.; Eryazici, I.; Jeong, N. C.; Hauser, B. G.; Wilmer, C. E.; Sarjeant, A. A.; Snurr, R. Q.; Nguyen, S. T.; Yazaydin, A. O.; Hupp, J. T. *J. Am. Chem. Soc.* **2012**, *134*, 15016.

(7) Hasell, T.; Schmidtman, M.; Cooper, A. I. *J. Am. Chem. Soc.* **2011**, *133*, 14920.

(8) Bushell, A. F.; Budd, P. M.; Attfield, M. P.; Jones, J. T.; Hasell, T.; Cooper, A. I.; Bernardo, P.; Bazzarelli, F.; Clarizia, G.; Jansen, J. C. *Angew. Chem., Int. Ed.* **2013**, *52*, 1253.

(9) Mitra, T.; Jelfs, K. E.; Schmidtman, M.; Ahmed, A.; Chong, S. Y.; Adams, D. J.; Cooper, A. I. *Nat. Chem.* **2013**, *5*, 276.

(10) Brutschy, M.; Schneider, M. W.; Mastalerz, M.; Waldvogel, S. R. *Adv. Mater.* **2012**, *24*, 6049.

(11) Hasell, T.; Schmidtman, M.; Stone, C. A.; Smith, M. W.; Cooper, A. I. *Chem. Commun.* **2012**, *48*, 4689.

(12) Schneider, M. W.; Oppel, I. M.; Griffin, A.; Mastalerz, M. *Angew. Chem., Int. Ed.* **2013**, *52*, 3611.

(13) Planas, N.; Dzubak, A. L.; Poloni, R.; Lin, L.-C.; McManus, A.; McDonald, T. M.; Neaton, J. B.; Long, J. R.; Smit, B.; Gagliardi, L. *J. Am. Chem. Soc.* **2013**, *130*, 7402.

(14) (a) Swamy, S. I.; Bacsá, J.; Jones, J. T. A.; Stylianou, K. C.; Steiner, A.; Ritchie, L. K.; Hasell, T.; Gould, J. A.; Laybourn, A.; Khimyak, Y. Z.; Adams, D. J.; Rosseinsky, M. J.; Cooper, A. I. *J. Am. Chem. Soc.* **2010**, *132*, 12773. (b) Culshaw, J. L.; Cheng, G.; Schmidtman, M.; Hasell, T.; Liu, M.; Adams, D. J.; Cooper, A. I. *J. Am. Chem. Soc.* **2013**, *135*, 10007.

(15) (a) Jin, Y.; Voss, B. A.; Jin, A.; Long, H.; Noble, R. D.; Zhang, W. *J. Am. Chem. Soc.* **2011**, *133*, 6650. (b) Jin, Y.; Voss, B. A.; Noble, R. D.; Zhang, W. *Angew. Chem., Int. Ed.* **2010**, *49*, 6348.

(16) Mastalerz, M.; Schneider, M. W.; Oppel, I. M.; Presly, O. *Angew. Chem., Int. Ed.* **2011**, *50*, 1046.

(17) Hasell, T.; Chong, S. Y.; Jelfs, K. E.; Adams, D. J.; Cooper, A. I. *J. Am. Chem. Soc.* **2012**, *134*, 588.

(18) Jelfs, K. E.; Eden, E. G.; Culshaw, J. L.; Shakespeare, S.; Pyzer-Knapp, E. O.; Thompson, H. P.; Bacsá, J.; Day, G. M.; Adams, D. J.; Cooper, A. I. *J. Am. Chem. Soc.* **2013**, *135*, 9307.

(19) (a) Jones, M. D.; Mahon, M. F. *J. Organomet. Chem.* **2008**, *693*, 2377. (b) Jurčík, V.; Wilhelm, R. *Tetrahedron: Asymmetry* **2006**, *17*, 801.

(c) Godin, G.; Levrant, B.; Trachsel, A.; Lehn, J. M.; Herrmann, A. *Chem. Commun.* **2010**, *46*, 3125. (d) Buchs née Levrant, B.; Godin, G.; Trachsel, A.; de Saint Laumer, J.-Y.; Lehn, J.-M.; Herrmann, A. *Eur. J. Org. Chem.* **2011**, *2011*, 681.

(20) Willems, T. F.; Rycroft, C. H.; Kazi, M.; Meza, J. C.; Haranczyk, M. *Microporous Mesoporous Mater.* **2012**, *149*, 134.

(21) Robeson, L. M. *J. Membr. Sci.* **1991**, *62*, 165.

(22) Vaidhyanathan, R.; Iremonger, S. S.; Shimizu, G. K.; Boyd, P. G.; Alavi, S.; Woo, T. K. *Science* **2010**, *330*, 650.

(23) Holden, D.; Jelfs, K. E.; Cooper, A. I.; Trewin, A.; Willock, D. J. *J. Phys. Chem. C* **2012**, *116*, 16639.

(24) Jorgensen, W. L.; Maxwell, D.; Tirado-Rives, J. *J. Am. Chem. Soc.* **1996**, *118*, 11225.

(25) (a) McKeown, N. B.; Budd, P. M. *Macromolecules* **2010**, *43*, 5163. (b) Ben, T.; Ren, H.; Ma, S. Q.; Cao, D. P.; Lan, J. H.; Jing, X. F.; Wang, W. C.; Xu, J.; Deng, F.; Simmons, J. M.; Qiu, S. L.; Zhu, G. S. *Angew. Chem., Int. Ed.* **2009**, *48*, 9457.